

APPLICATION OF LIGHT LATTICE STRUCTURES FOR GAS TURBINE ENGINE FAN BLADES

L. Magerramova, M. Volkov, A. Afonin, M. Svinareva, D. Kalinin
Central Institute of Aviation Motors named after P.I. Baranov

Keywords: *lattice structures, gas turbine, fan blades*

Abstract

One of the main tasks in designing units and parts of gas turbine engines for aircrafts is to achieve a minimum mass while meeting the requirements of strength reliability and durability.

The problem of increasing weight efficiency can be solved using optimal design of structures by dint of modern optimization methods, and further manufacture of such structures is possible due to the use of advanced technologies.

The article presents the results of numerical and experimental investigation of cellular structures and the constructions of hollow fan blades for gas turbine engine with various internal structures intended for manufacturing by additive production methods.

1 Introduction

The fan blade for gas turbine engine is a massive part subjected to centrifugal forces, airflow pressure. Foreign object damage and flutter are significant damaging factors.

Various optimization methods, including topology optimization, are used in a number of industries designing lightweight, robust and reliable structures. Manufacturing of created designs can often be carried out only through additive technologies.

Additive technologies allow to apply unique opportunities for production of parts with complex geometry, and the interaction of additive manufacturing and optimization makes it possible to implement original solutions of designers respecting the requirements of structural continuity and strength of structures.

One of the advantages of additive manufacturing is the possibility of producing solid bodies of almost any complex shape. With respect to the details of gas turbine engines, the ability to create technologically complex shapes of parts allows to reduce the weight of parts and components, such as the vanes and blades of the compressor. Due to additive technologies, it is possible to make lightweight structures by creating cavities in them. In this case, the load-bearing capacity of the structure can be achieved by constructing reinforcing elements in the cavity, such as lattices, cellular, porous structures.

The cellular / lattice structures endure significant deformation without destruction and are resistant to fatigue.

2 Cellular and lattice constructions and manufacturing methods

Various schemes for filling cavities in blades with lattice or other structures are proposed. For example, in [1] the construction of a hollow compressor guide vane is proposed. The walls forming gas-dynamic contours of the blade and internal cellular structure are made simultaneously by the methods of additive technologies. The thickness of the bridges (40 in Figure 1a) forming cellular structure can be from 10 to 80 percent of thickness of the walls of the blade. The blade can be filled up to 75% of the volume by cellular structure. In this case, the dimension of the honeycomb structure can vary along the height of the blade and in cross section plane. This technology can be applied for the manufacturing of both stator and rotor compressor blades. The use of this approach

allows reducing the weight of the blade significantly without losing its strength properties.

Design models with various fillers have been designed and manufactured by additive technologies (Figure 1).

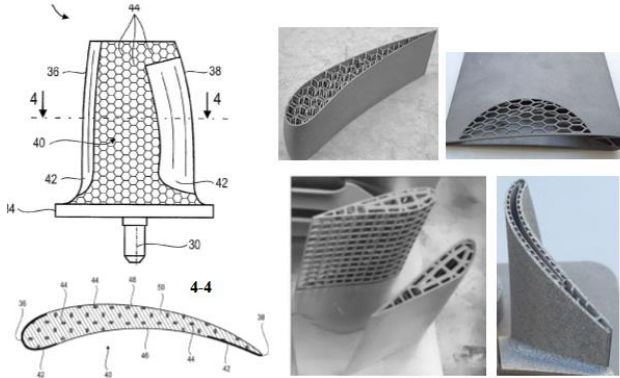
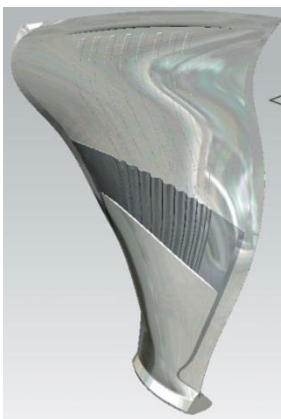


Fig.1 a) Example of the filling cavities in blades and b) fragments of printed lattice structures

Technologies for the production of lattice and cellular structures are currently being developed by various enterprises [2].

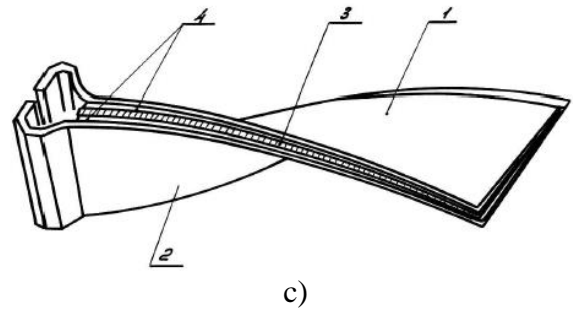
A wide-chord fan blade of a titanium alloy sheet with a filling of the cavity in the form of a corrugation was developed (Figure 2a). The mass was reduced by 37% in comparison with the completely filled structure [3]. The manufacturing of the blade is based on the combination of diffusion welding techniques and superplastic forming. The Rolls-Royce Company uses the same method to produce hollow fan blade of the third generation (Fig. 2b).



a)



b)



c)

Fig.2 Wide-chord fan blades with cavity fillers: a, b) corrugation, c) cellular structure




Figure 2c shows a three-layered blade with a honeycomb core, obtained by bonding the elements of the airfoil (1, 2) from the stamped titanium sheet and the honeycomb filler (3) made of titanium foil by explosion energy molding, and gaskets (4) between them made of high-temperature solder.

3 Research of cellular structures

Cellular / lattice structures are recently of greater interest [3-8]. Experimental studies of panels of high-temperature nickel alloys in IN-718 and Mar-M247 [5] have shown that lattice structures are more resistant to defects than honeycomb structures. In [6], the expediency of using cellular structures of various densities made of titanium alloy by the SLM method was studied by the analysis of their properties.

Here, several variants of structures were chosen to identify the characteristics of cellular structures, for which numerical and experimental research have been carried out. The designed flat samples are made of powder (10-40 microns) of titanium alloy CL41 Ti (Ti6Al4V) by selective laser melting (SLP) on the *Concept Laser M2 Cusing SingleLaser 400W*. Software: Materialize Magics. Melting modes: layer thickness - 25 microns; Laser power (max.) - 200 W; melting trajectory of planes - meander; segmentation of planes into segments - 5x5 mm, displacement of 1 mm along the X and Y axes on each layer; pseudo-random melting order. To print selected structures, the Structures module in Materialize Magics is used.

Table 1 - Samples and characteristics of the cellular structures

Structure type	Name	Designations of structures	t , mm	a , mm	Element section configuration	Designations of samples	$K\rho$
#1 	Rhombic dodecahedron RD20 (4-4-4)	RD4	0,6	4	circle	1-1, 1-2	0,19
#2 	Rhombic dodecahedron D20 (3.5-3.5-3.5)	RD3.5	0,5	3,5	circle	1-3, 1-4	0,19
#3 	Dodecahedron DM (3.5-3.5-3.5)	DM3.5	0,4	3,5	triangle	1-5, 1-6	0,13

Here, t is the typical thickness of the element, a is the distance between the nodes, $K\rho$ is the relative density.

After the samples were made in an argon medium, heat treatment was performed with the following parameters: heating to 840 ° C for 4 hours, maintaining the temperature for 2 hours, and then cooling in the furnace to 500 ° C.

4 Tensile tests of the samples

Figure 3 shows a drawing and model of a sample with cellular structures for tensile tests.

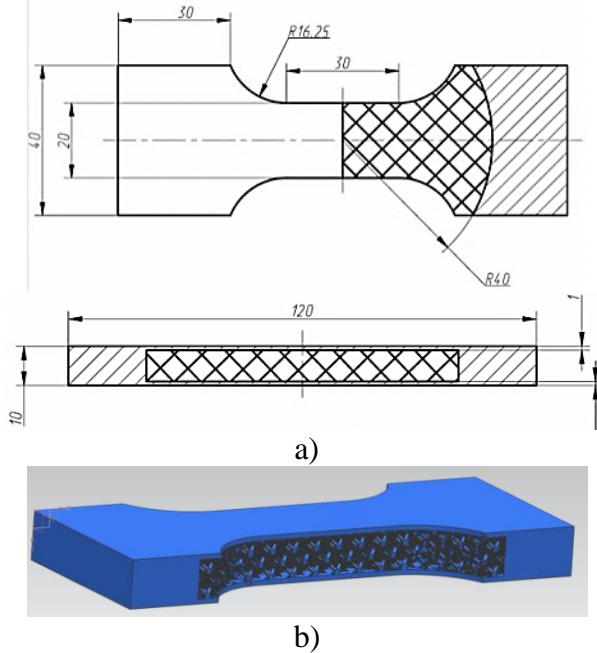


Fig.3 Lattice structure sample for tensile tests: a) drawing, b) model

Figure 4 shows photographs of samples with different structures. The width of the working

part $a_0 = 20\text{mm}$, the total thickness $b_0 = 20\text{mm}$, the thickness of the plates $t_0 = 1\text{mm}$. The geometric (nominal) cross-sectional area of the working part of the sample is $S_0 = 200\text{mm}^2$, the area of cellular part is $S_{\text{cel}} = 160\text{mm}^2$.

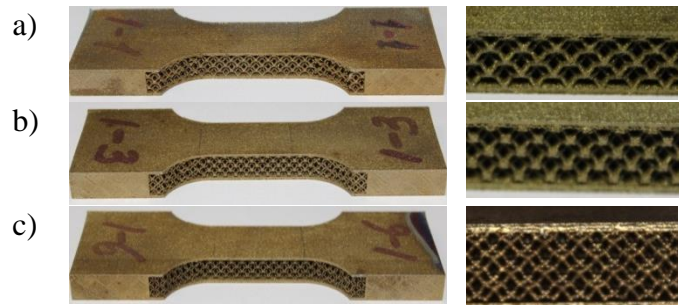
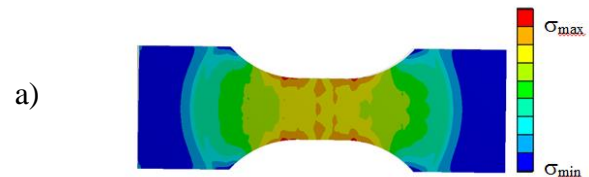


Fig.4 Samples from CL41 Ti (Ti6Al4V) with different cell structures and enlarged fragments: a) # 1-RD4, b) # 2-RD3.5, c) # 3- DM3.5

Numerical experiments were performed for tensile tests of cellular structures. To determine the destructive loads, the sample was stretched by different forces to achieve local stresses corresponding to values slightly exceeding the ultimate strength of the foundry titanium alloy. The results of calculations are shown in figures 5-7.



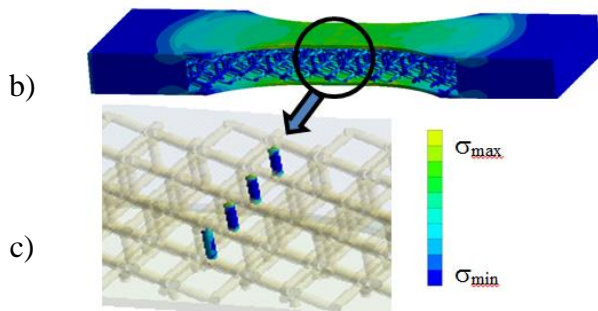


Fig.5 Von Mises stress in a sample of RD4 ($a = 4$ mm, $t = 1$ mm) when loaded with force ~ 30 kN: a) in the plate, b) in the sample, c) in the cells (fragment)

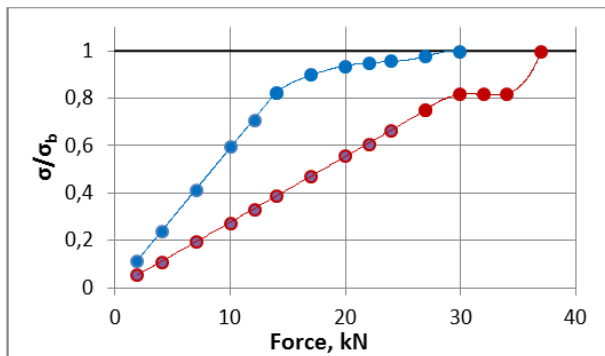


Fig.6 Dependence of the maximum relative stress in the plate (blue line) and cellular structure (red line) on the applied force for sample RD3.5

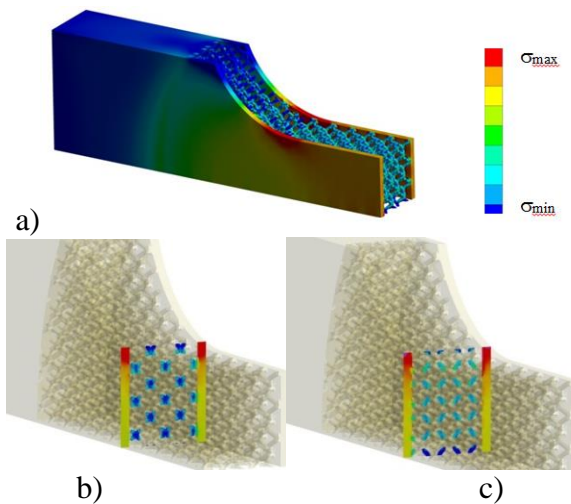


Fig.7 Von Mises stress (MPa) in the sample RD3.5 with a load of ~ 30 kN: a) in the plate zone, b) in the cross section along the nodes, c) along the elements of the lattice rods

The values of calculated damaging loads with relative value of maximum stress equal to 1 for the plates and lattice part of the sample RD3.5 are ~ 30 kN and 37.5 kN, respectively. The values of the maximum stress in the plates are higher than in the cells. Stress in the nodes of the lattice is less than in the cross sections of the rods.

Tensile tests of special samples with a lattice structure were carried out in the laboratory of CIAM, certified and accredited by Interstate Aviation Committee (IAC) (accreditation certificate No. IL-128 - valid until 03.10.2021). The moving speed of the movable gripper of the test machine is $V = 0.3$ mm / min. Tests of mechanical characteristics were carried out in accordance with [9].

The values of the experimental ultimate loads were observed in the range from 36.7 to 45.0 kN, which is close to calculated values. All the samples collapsed in the transition zone from the working part to the fillet. Apparently, this was facilitated by the concentration of stress in this zone. Thin plates are destroyed first. The cellular structure continues to deform and collapses later. The computational simulation showed the same type of stress distribution (Figure 5 -7).

According to [9], when determining the mechanical characteristics, the cross-sectional area of the working area of the sample is used. For a cellular sample, the area that receives the load is the sum of the cross-sectional areas of the plates (S_{pl}) and the structural cellular elements of the section, taking into account their relative density ($S_{cel} \cdot K_p$). Figure 8, 9 shows test results and photographs of samples.

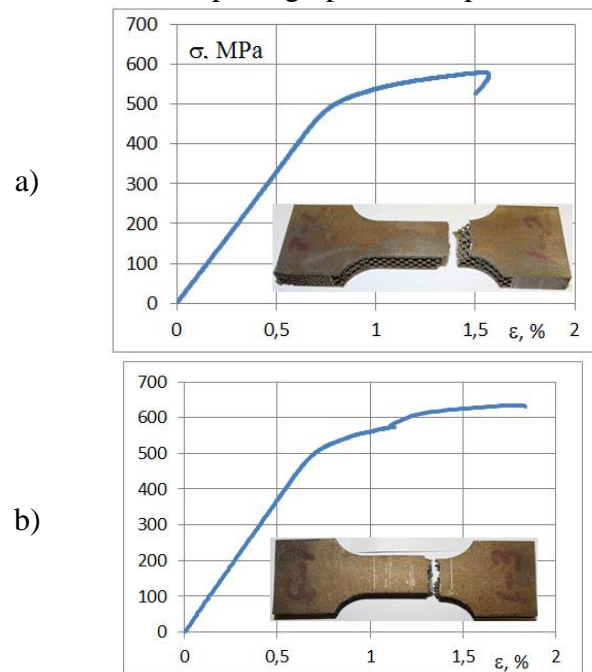


Fig.8 Test results of the samples: a) #1-2 (RD4), b) #1-3 (RD3.5)

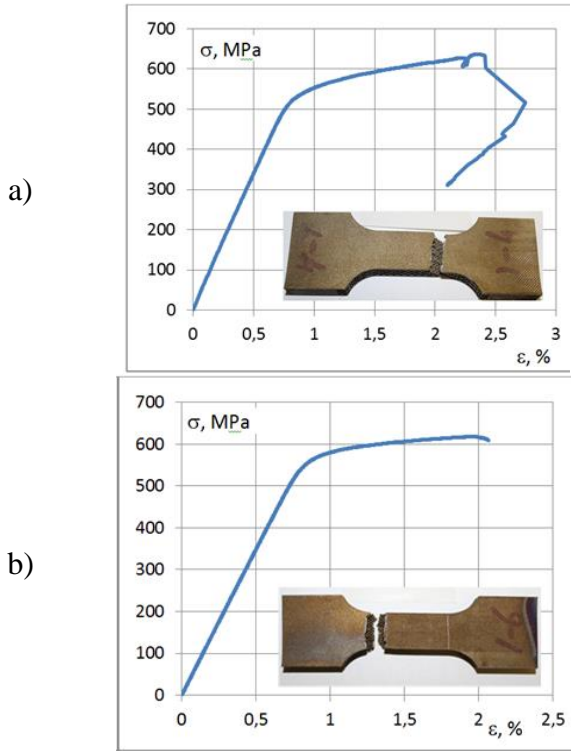


Fig.9 Test results of the samples: a) #1-4 (RD3.5), b) #1-6 (DM3.5)

Table 2 - Mechanical properties obtained from the results of testing the samples with cellular structure for tensile at room temperature

№	Type	P_{max} , kN	S_r , mm ²	$E(S_r)$, GPa	$\sigma_{0.2}(S_r)$, MPa	σ_B (S_r), MPa	ψ , %	δ , %
1-1	#1	36,7	71,07	69,34	484,06	516,43	3,49	1,12
1-2	#1	41,1	70,97	65,72	540,78	579,12	2,12	0,46
1-3	#2	45,0	70,84	73,96	554,64	635,26	2,71	1,51
1-4	#2	44,8	70,32	67,25	553,59	637,05	1,15	2,61
1-5	#3	39,4	60,89	74,14	590,33	647,06	3,17	2,76
1-6	#3	37,8	61,23	69,63	584,16	617,35	5,49	1,76
VT6*	-	-	-	115	804	882	12	5

(*) Data from the reference book for the foundry alloy VT6, obtained by stretching samples from a solid material.

Here P_{max} , kN - maximum load; S_0 , mm² - geometric cross-section area; S_r , mm² - the cross section area for the load capacity; E , GPa - elastic modulus; $\sigma_{0.2}$, MPa - yield strength; σ_B , MPa - ultimate strength; ψ , % - reduction of area; δ , % - elongation.

The mechanical characteristics of the cellular material, referred to the geometric area of the sample cross-section, are lower than for solid cast material, as expected. However, the density of the cellular structure is much lower. This allows one to win in the mass of the

structure. Table 3 shows the relative characteristics of mesh samples in tensile tests, calculated taking into account the nominal and real cross-sectional area.

Table 3 - Relative mechanical properties of tested samples with different structures, calculated using the nominal and real cross-sectional area

Type of sample	K_δ	K_ψ	K_E	K_{σ_b}	$K_{\sigma_{0.2}}$	K_{σ_p}
#1	0,16	0,23	0,55	0,62	0,64	1,76
#2	0,41	0,16	0,61	0,72	0,69	2,05
#3	0,45	0,36	0,62	0,72	0,73	2,36
Average Kmp	0,34	0,25	0,61	0,69	0,69	-

Here K_E , K_{σ_b} , $K_{\sigma_{0.2}}$, K_δ , K_ψ are the ratios between the average mechanical properties obtained in testing cellular tensile samples calculated from the load-bearing cross-sectional area (S_r).

$K_{\sigma_p} = K_{\sigma_b}/K_p$ is the relative strength on the bearing area. Kmp – average values of relative characteristics for all types of samples.

These results can be explained as follows. For example, for a type # 3 sample, the tensile strength calculated from the section bearing area is 72% of the strength of the solid material, and the mass is 13% of the solid material. I.e. in the "strength / mass" ratio, the gain of the mesh sample compared with the solid sample is ~2,36 times. For different types of cellular structures, these parameters are different.

The obtained results can be used in calculations of parts with cellular structures.

5 Calculations of the fan blade

To describe large and complex parts with cellular structures by finite element methods, it is necessary to form models with a huge number of finite elements, which requires large memory resources and computer processing speed. To reduce the amount of memory and reduce the calculation time, it is proposed to replace a part of the structure consisting of cellular structures with a continuous equivalent material with density ($\rho^* = \rho K_\rho$) and elastic modulus ($E^* = E \cdot K_E$), corresponding to the original cellular structure. We can use the results

obtained above on the basis of cellular tensile tests to determine these parameters.

As an example, a hollow fan blade is considered (Fig. 10a). The thickness of the walls of hollow blades in the root zone is 2 mm, on the periphery - 1 mm. The volume of the blade with the cavity is $\sim 76\%$ of the continuous blade. The cavity of the blade is filled with various structural elements (Figure 10b-10d).

The blade is loaded with centrifugal and gas forces. Rotational speed 4000 rpm, average pressure of gas forces 0.035 MPa.

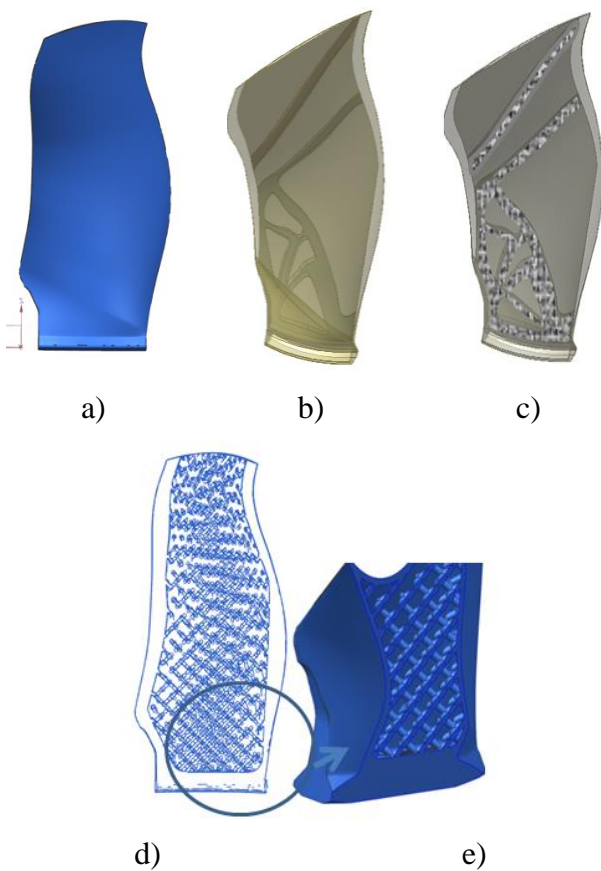


Fig.10 Models of fan blades: a) solid (#1), b) with lattice (#2), c) lattice-cellular (#3-#5) and d) cellular structures (#6-#8), e) a fragment of cellular structure

Figure 11 shows the distribution of von Mises and radial stress in the hollow blade #6, filled with an imitation of the cellular structure RD4 ($K_p=0,19$ и $0,55$).

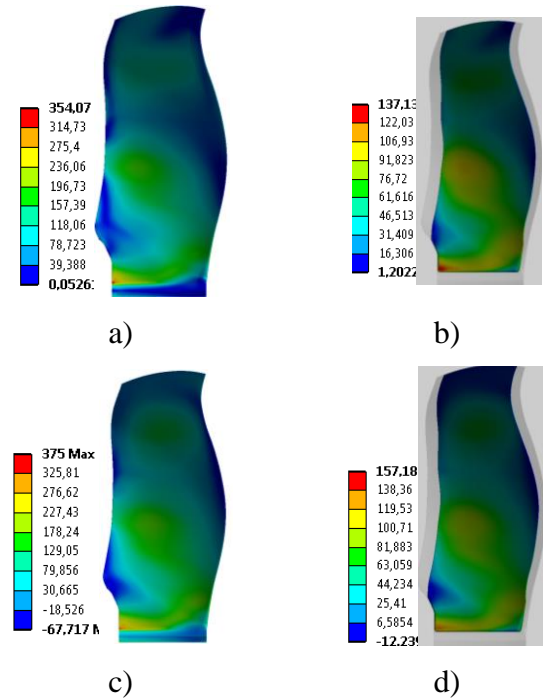


Fig.11 Stress field (MPa) of the blade #6: a) von Mises in the shell b) von Mises in the internal structure, c) radial in the shell, d) radial in the internal structure

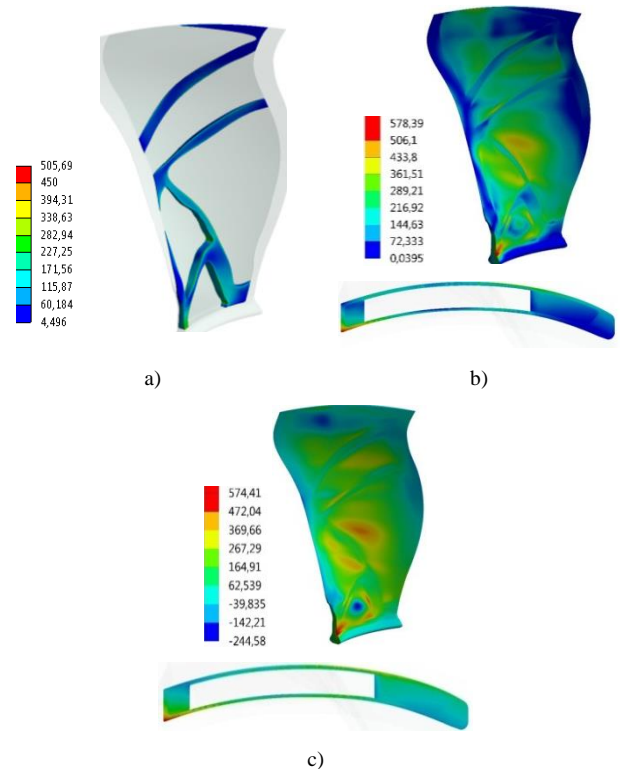


Fig.12 Stress field (MPa) of blade #3 a) von Mises stress in the lattice structure, b) von Mises stress and c) radial in the blade and in sections passing through the zone with maximum stress

The maximum radial and von Mises stress occurs in the area of the fillet between the profile part and the shank.

Table 4 shows the calculations of maximum von Mises stress, radial stress and natural oscillation frequency of the considered blades under operating conditions at 4000 rpm. Blades number 2-5 are latticed. Blade #2 contains lattice made of solid material (Fig. 10b). For blades #3-5 (Figure 10c), the lattice consist of cellular structures with relative density and relative elastic modulus parameters given in Table 4. The cavities of the blades #6-8

are completely filled with cellular structures with the same parameters as for blades #3-5 respectively.

The gain in mass of the blades with cellular structures was from 27 to 64% in comparison with a continuous one. At the same time, the maximum stress in the "dangerous" zones of fillets between the profile part and the shank in the examined blades #6-8 with cellular structures are almost two times less than in the continuous blade.

Table 4 - Results of calculation of fan blade variants with different structures

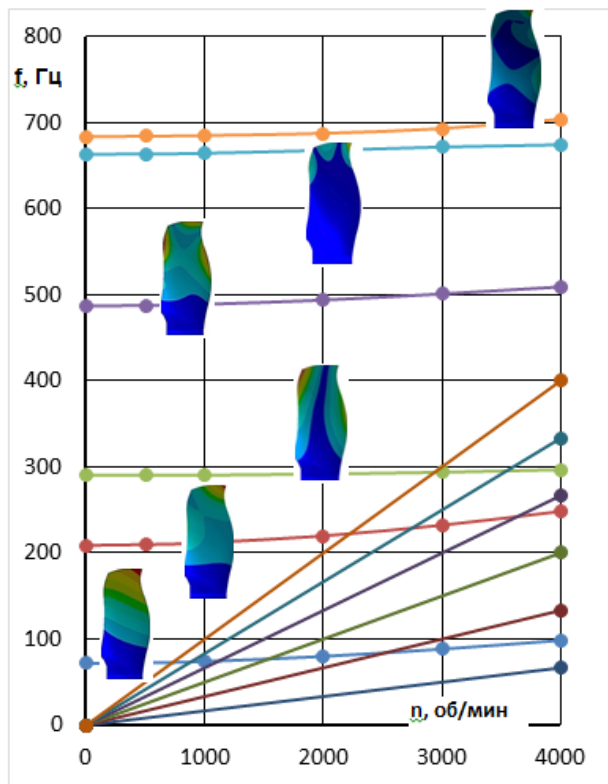
Blade variant №	Parameter	solid	lattice	lattice-cellular			RD4	RD3.5	DM3.5
		1	2	3	4	5	6	7	8
	K_E	1	1	0,55	0,61	0,62	0,55	0,61	0,62
	K_ρ	1	1	0,19	0,19	0,13	0,19	0,19	0,13
	Max σ_{mis} , MPa	622,67	600,8	578,39	564,15	556,49	354,07	340,72	326,01
	Max σ_Y , MPa	707, 63	597,25	574,41	560,38	552,80	375,00	371,63	349,47
Natural	f1	85,21	87,70	90,47	90,72	68,15	98,47	99,58	102,58
	f2	208,63	199,36	208,17	208,98	181,68	248,44	251,90	261,08
	f3	256,76	233,93	231,69	232,22	206,06	296,75	302,33	311,62
	f4	429,17	337,42	318,24	319,52	350,67	509,17	518,18	535,74
	f5	578,52	410,22	379,81	381,18	422,98	674,27	686,21	704,07
	f6	616,72	416,61	428,21	429,74	487,64	704,02	716,86	743,08
	Weight, kg	13,53	6,40	4,91	4,91	4,80	9,83	9,83	9,56
	Gain, %	-	52,7	63,7	63,7	64,5	27,3	27,3	29,3

In lattice and cellular-lattice blades #2-5, the maximum von Mises stress are up to 10%, and the radial ones are 16 to 22% lower than in the continuous blade.

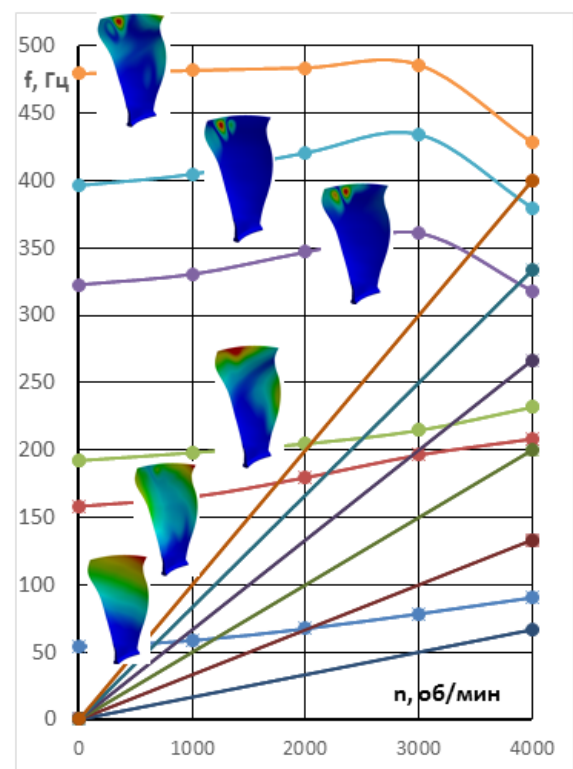
Figure 13 shows the Campbell diagrams for the first six waveforms of the designed #6 (a) and #3 (b).

All blades with the exception of #2 and 8 do not have resonances with respect to the first six natural forms of oscillation. For blades #2 and #8, resonances are possible with respect to the second eigenmodes of oscillations with excitation harmonics $k = 3$ and $k = 4$, respectively, which is inadmissible.

The values of natural oscillation frequencies of blades with lattice structures are lower than those of blades completely filled with certain structures. This difference is especially great in frequencies above the 3rd form. Forms of oscillations in 4, 5 and 6 differ significantly from the forms of oscillations of uniformly filled blades. Plate-shaped oscillations of the peripheral parts of the blades predominate because of their design (Figure 13a).



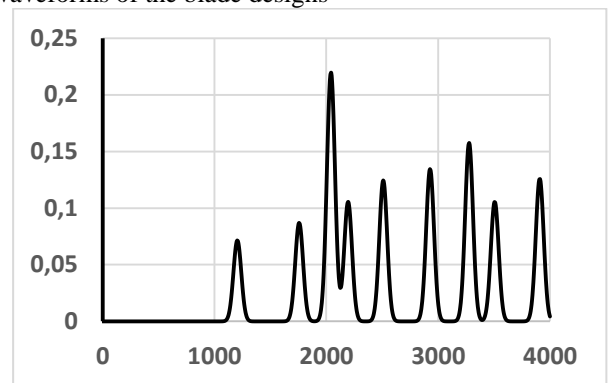
a) blade #6



b) blade #3

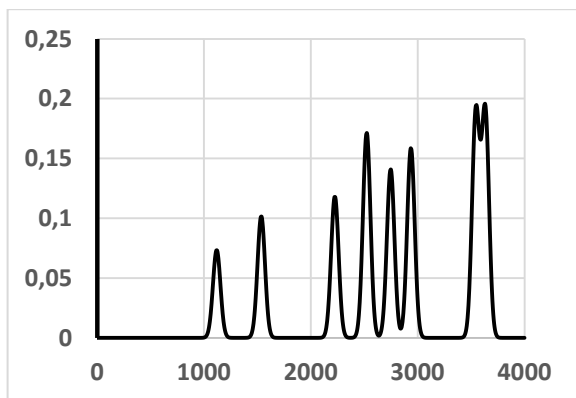
Fig.13 Campbell diagrams for the first six waveforms of the blade designs

Figure 14 shows the distribution of the probability density ($p, \%$) of the appearance of a resonance per unit time in the operating frequency range: 1000..4000 rpm. The amplitudes of the oscillations were used in a relative form. The graph built in the assumption of vibration damping and with a linear increasing angular speed of the rotor. Taking into account the flight schedule of the aircraft, the probability of resonance in the high-speed zone (cruising mode) will increase significantly.



b) blade №3

Fig.14 Density of probability of a resonance in the operating speed range



a) blade №6

The application of the diagram makes it possible to determine the most dangerous zones of the mutual influence of resonances of different shapes and frequencies. In particular, the greatest probability of occurrence of a resonance in the considered blades is revealed in the blade No. 3 at a frequency of 2041 rpm and does not exceed 0.22%.

Production of blades with cellular structures

Production of blades with cellular structures is impossible by traditional methods. It is possible to use layer-by-layer selective laser sintering / fusion (SLS) methods. After the manufacturing of the blades, heat treatment, cutting off the supports, removing the products from the platform and removing the excess powder from the cavities of the blades are necessary. The obtained parts with a complex internal structure should be improved according to the possibility of their production by additive methods. In the designs of blades intended for the production by layer-by-layer methods, openings must be provided to remove powder residues from the cavities. These holes can be placed on the shoe sole and / or on the end of the blade.

To determine the possibility of manufacturing hollow blades by the SLS method, a reduced blade model with filler cavity in the form of a corrugation (Figure 15b) was prepared from a powdered titanium alloy CL41 Ti (manufactured by Concept Laser, Germany), which is an analogue of a titanium alloy of Russian production (VT6). The particle size of the powder is from 10 to 40 μm .

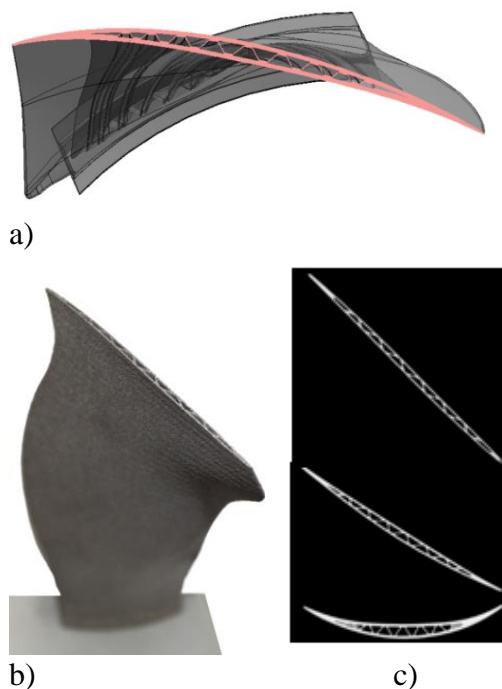


Fig.15 Fan blade with a filler in the form of corrugation: a) a fragment of the model, b) a printed blade of titanium alloy, c) a tomogram of sections

Tomographic images of the cross sections along the height of the blade are made on the XT H 225 X-ray and CT inspection of the company SOVTEST ATE (Figure 15c). Tomographic analysis has shown that the structure corresponds to a given three-dimensional model (Figure 15a).

The model was printed using the SLA method of polymer (Figure 16a) and SLM of the titanium alloy CL41 Ti (Figure 16b, c). The cellular structure is clearly visible in the polymeric structure of the blade.

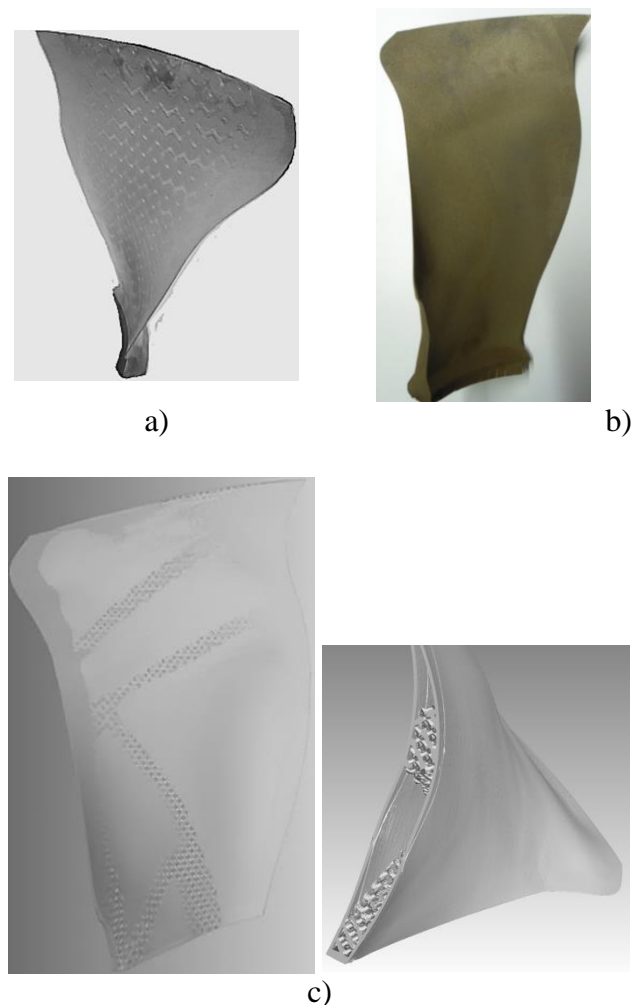


Fig.16 Fan blade with a cellular filler: a) a printed blade of polymer, b) a printed blade of titanium alloy, c) tomograms

All models were printed by Nissa Digispace on the Concept Laser plants.

Conclusion

Flat titanium samples formed by flat plates between which the cellular structures are

located are considered. Calculations and experimental studies of the stress state changes in the elements of the samples under the action of tensile loads are carried out. The values of the experimental and calculated loads destroying the sample are in good agreement with each other. It is found out that the stress in the plates reach the values of the tensile strength a little earlier than in the cellular structures.

Based on these studies, for the three different types of cellular structures, the mechanical characteristics of the structures examined are determined. It was found that the "strength / mass" ratio of the examined cellular samples is 1,76 – 2,36 times greater than that of solid.

These characteristics were used in the calculation of hollow blades with cellular fillings. The weight of such blades is 27-64% less than at all-metal blade and the stress in the "dangerous" zones are 2 times less.

The possibility of manufacturing hollow blades with various cellular structures is verified by the method of printing SLA and SLM from titanium alloy. Tomographic studies have shown that the structures correspond to the given three-dimensional models.

When designing parts to reduce their mass, cellular structures should be placed in low-loaded areas of the structure and in zones of compressive influences.

The most proper models are #4-#7.

structures.

http://www.tms.org/superalloys/10.7449/2004/Superalloys_2004_431_439.pdf

- [6] Sabina L. Campanelli, Nicola Contuzzi, Antonio D. Ludovico, Fabrizia Caiazzo, Francesco Cardaropoli, Vincenzo Sergi. Manufacturing and Characterization of Ti6Al4V Lattice Components Manufactured by Selective Laser Melting. *Materials* 2014, 7, 4803-4822; doi:10.3390/ma7064803. ISSN 1996-1944 www.mdpi.com/journal/materials.
- [7] L.A.Magerramova, M.S. Svinaryova, A.S. Siversky, M.E Volkov. Cellular Structures Produced by Additive Technologies for GTE Components. *Technology of Light alloy*, No3, pp 24-35, 2017.
- [8] Magerramova L., Volkov M., Svinareva M., Siversky A. The use of additive technologies to create lightweight parts for gas turbine engine compressors. *Proc. ASME TurboExpo* 2018, GT2018-75904
- [9] Metals. Methods of tension test, GOST 1497-84, ISO 6892-84.

Copyright Statement

The authors confirm that they, and/or their company or organization, hold copyright on all of the original material included in this paper. The authors also confirm that they have obtained permission, from the copyright holder of any third party material included in this paper, to publish it as part of their paper. The authors confirm that they give permission, or have obtained permission from the copyright holder of this paper, for the publication and distribution of this paper as part of the ICAS proceedings or as individual off-prints from the proceedings.

References

- [1] Pat. 2015/0064015 A1 US. Composite blade made by additive manufacturing Pub. Date Mar. 5, 2015.
- [2] R. V. Safiulin/ Superplastic forming and pressure welding of multilayer hollow structure. *Part 1. International experience. Institute for Metals Superplasticity Problems RAS. Letter of materials*. Vol. 2, pp 32-35, 2012. <http://www.lettersonmaterials.com>
- [3] S.I. Molodex, V.V. Tretiyk. Development of technology for the manufacture of hollow wide-chord fan blades Turbofan. *Technology of aircraft production*, pp. 10-14, 2008.
- [4] N.E. Kablov, V.A. Skibin, U.A. Abysin, V.N. Kochetov, A.A. Shavnev, T.D. Karimbaev, A.A. Luppov. Wide-chord fan blades for 5-6th generation Turbofan. *Conversion in mechanical engineering*. No 5, pp. 5-16, 2006.
- [5] M.V. Nathal, J.D. Whittenberger, M.G. Hebsur, P.T. Kantzos, and D.L. Krause. Superalloy lattice block